HAL
open science

Vulnerability to cavitation in Olea europaea current-year shoots: further evidence of an open-vessel artifact associated with centrifuge and air-injection techniques

Jose Manuel Torres Ruiz, Hervé Cochard, Stefan Mayr, Barbara Beikircher, Antonio Diaz-Espejo, Celia M. Rodriguez-Dominguez, Eric Badel, José Enrique Fernandez

▶ To cite this version:

Jose Manuel Torres Ruiz, Hervé Cochard, Stefan Mayr, Barbara Beikircher, Antonio Diaz-Espejo, et al.. Vulnerability to cavitation in Olea europaea current-year shoots: further evidence of an open-vessel artifact associated with centrifuge and air-injection techniques. Physiologia Plantarum, 2014, 152 (3), pp.465-474. 10.1111/ppl.12185 . hal-01123401

HAL Id: hal-01123401

https://hal.science/hal-01123401v1

Submitted on 16 Mar 2018

HAL is a multi-disciplinary open access archive for the deposit and dissemination of scientific research documents, whether they are published or not. The documents may come from teaching and research institutions in France or abroad, or from public or private research centers.

L'archive ouverte pluridisciplinaire **HAL**, est destinée au dépôt et à la diffusion de documents scientifiques de niveau recherche, publiés ou non, émanant des établissements d'enseignement et de recherche français ou étrangers, des laboratoires publics ou privés.

Vulnerability to cavitation in *Olea europaea* current-year shoots: further evidence of an open-vessel artifact associated with centrifuge and air-injection techniques

José M. Torres-Ruiz[a,*], Hervé Cochard[b,c], Stefan Mayr[d], Barbara Beikircher[d], Antonio Diaz-Espejo[a], Celia M. Rodriguez-Dominguez[a,e], Eric Badel[b,c] and José Enrique Fernández[a]

[a]Irrigation and Crop Ecophysiology Group, Instituto de Recursos Naturales y Agrobiología de Sevilla (IRNAS, CSIC), Avenida Reina Mercedes, No. 10, Sevilla, 41012, Spain
[b]INRA, UMR547 PIAF, Clermont-Ferrand, 63100, France
[c]Clermont Université, Université Blaise-Pascal, UMR547 PIAF, BP 10448, Clermont-Ferrand, 63000, France
[d]Department of Botany, University of Innsbruck, Sternwartestr. 15, Innsbruck, A-6020, Austria
[e]Departamento de Biología Vegetal y Ecología, Universidad de Sevilla, Avda. Reina Mercedes 6, Sevilla, 41012, Spain

doi:10.1111/ppl.12185

Different methods have been devised to analyze vulnerability to cavitation of plants. Although a good agreement between them is usually found, some discrepancies have been reported when measuring samples from long-vesseled species. The aim of this study was to evaluate possible artifacts derived from different methods and sample sizes. Current-year shoot segments of mature olive trees (*Olea europaea*), a long-vesseled species, were used to generate vulnerability curves (VCs) by bench dehydration, pressure collar and both static- and flow-centrifuge methods. For the latter, two different rotors were used to test possible effects of the rotor design on the curves. Indeed, high-resolution computed tomography (HRCT) images were used to evaluate the functional status of xylem at different water potentials. Measurements of native embolism were used to validate the methods used. The pressure collar and the two centrifugal methods showed greater vulnerability to cavitation than the dehydration method. The shift in vulnerability thresholds in centrifuge methods was more pronounced in shorter samples, supporting the open-vessel artifact hypothesis as a higher proportion of vessels were open in short samples. The two different rotor designs used for the flow-centrifuge method revealed similar vulnerability to cavitation. Only the bench dehydration or HRCT methods produced VCs that agreed with native levels of embolism and water potential values measured in the field.

Introduction

The plant water transport capacity through xylem is one of the most important aspects in plant–water relations. The xylem hydraulic conductance (k, $kg\,s^{-1}\,MPa^{-1}$) is highly variable as cavitation can disconnect the water columns under tension (Franks and Brodribb 2005). Cavitation, i.e. the change from liquid to water vapor induced by 'air-seeding' (Tyree and Zimmermann 2002), breaks the water columns in the xylem conduits at specific tensions and, in consequence, reduces plant water transport capacity. Vulnerability curves (VCs) relate a xylem segment's change in k to its xylem tension and show the percent loss of conductance (PLC) from full saturation to low water potentials (Ψ, MPa) (Sperry et al. 1988). Accurate VCs are, therefore, crucial for a proper understanding of the plant resistance to low xylem Ψ (Ψ_x, MPa), i.e. high xylem tensions.

Abbreviations – HRCT, high-resolution computed tomography; PLC, percent loss of conductance; VCs, vulnerability curves.

A common method for generating VCs is by bench dehydration in which plants are gradually dehydrated and the PLC and corresponding Ψ_x are determined in intervals (Sperry and Tyree 1988, Tyree and Zimmermann 2002). As it is time consuming, faster methods have been developed to induce and analyze cavitation (see Cochard et al. 2013 for a review). The pressure collar method is based on inducing air entry into conduits by the use of a double-ended pressure sleeve or a pressure chamber containing a xylem segment (Cochard et al. 1992, Salleo et al. 1992, Sperry and Saliendra 1994, Tyree and Zimmermann 2002, Mayr et al. 2006). The static-centrifuge method is based on the generation of different xylem tensions in the mid-points (axis of rotation) of samples by spinning at different velocities in a custom-built rotor (Pockman et al. 1995, Alder et al. 1997). Cochard (2002), Cochard et al. (2005) and Li et al. (2008) modified the static-centrifuge method and developed new rotor designs that allowed determining *k* during spinning (flow-centrifuge method). Both rotors are based on the same principle, but designs differ in some details (e.g. water delivery to the reservoirs during spinning; Sperry et al. 2012).

Although the bench dehydration has been typically considered as the 'gold standard' method for generating true physiological VCs (Cochard et al. 2010, Sperry et al. 2012), its reliability has been recently questioned due to possible blockages of the xylem conduits during the dehydration process or sampling artifacts that would affect the PLC measures (Jacobsen and Pratt 2012, Wheeler et al. 2013). The pressure collar and the two centrifuge methods have been validated in different studies for several angiosperm species with different xylem characteristics (Alder et al. 1997, Li et al. 2008, Taneda and Sperry 2008, Jacobsen and Pratt 2012, Sperry et al. 2012). However, it has also been suggested that they may be problematic for obtaining accurate VCs in case of long-vesseled species. Ennajeh et al. (2011) reported an overestimation of vulnerability thresholds when VCs were generated by double-ended pressure sleeves from xylem segments shorter than the species' maximum vessel length. Choat et al. (2010) and Cochard et al. (2010) reported overestimated vulnerabilities by using the static- and flow-centrifuge methods, respectively, when the xylem segments showed a high proportion of open vessels at both ends. More recently, McElrone et al. (2012) demonstrated by the use of high-resolution computed tomography (HRCT) that centrifuge methods overestimate vulnerability to cavitation in grapevines (*Vitis vinifera*). Contrasting results have even been reported for the same species and its population when the sample length was varied (Cochard et al. 2010, Sperry et al. 2012), whereby these differences attributed to the centrifuge rotor design.

The aim of this study was to compare VCs generated by bench dehydration, pressure collar and static- and flow-centrifuge methods on identical samples to test the possible open-vessel artifacts (Choat et al. 2010, Cochard et al. 2010) and the possible influences of the rotor design. HRCT was used to obtain images of the xylem vessels of dehydrated samples at different Ψ_x to evaluate the functional status of xylem. Measurements of native embolism were also carried out and their results compared with the curves generated with all the methods compared (Charra-Vaskou et al. 2012, Brodersen et al. 2013). All samples were from olive (*Olea europaea* cv. Manzanilla), a long-vesseled and very drought and cavitation-resistant species (Ennajeh et al. 2008). All curves were generated by using current-year shoots in order to avoid possible effects of cavitation fatigue (Hacke et al. 2001).

Materials and methods

Experimental site and growth conditions

All samples were harvested from ca. 42-year-old olive trees grown in 'La Hampa' experimental farm, 15 km from Seville, southwest Spain (37°17′N, 6°3′W, 30 m a.s.l.). Climate in the area is Mediterranean with a wet, mild season from October to April and a hot, dry season from May to September. All trees were irrigated daily during the irrigation season (from May to October) with 100% of the crop evapotranspiration (ET_c) to maintain them under well-watered conditions. The irrigation doses were calculated according to the crop coefficient approach (Allen et al. 1998), with coefficients adjusted for the orchard conditions by Fernández et al. (2006). Although the samples used in this study (except for the HRCT) were collected at different times from July to September 2010, they can be considered as homogenous plant material as the development of the current-year shoot of olive trees starts in March and stops at the end of June (Barranco et al. 1998, Pastor 2005). Samples for the HRCT were collected in February 2013.

Sample collection and preparation for *k* measurements

A common protocol was used for collecting and preparing the samples for *k* measurements. Briefly, 1.25-m-long branches from different representative trees were cut under water (to avoid air entering into the vessels), wrapped into plastic bags with wet paper towel inside (to prevent transpiration) and transported to the laboratory. Once in the laboratory, current-year shoots

were excised under water from the collected branches and, then, segments of different lengths (depending on the methods) were also cut under water from the shoots. The multiple cuts under water and prevention of transpiration of the current-year shoots would have ensured that cutting artifacts as described in Wheeler et al. (2013) were avoided. In those cases in which *k* was determined by using the XYL'EM® apparatus (Bronkhorst, Montigny-les-Cormeilles, France), samples were previously debarked, their ends were trimmed with a razor blade and then plugged to such device for *k* measurements.

Native xylem water potential and embolism

The Ψ_x of current-year shoots was determined at 11:30 GMT in two leaves per shoot of six representative trees with a Scholander-type pressure chamber (Soilmoisture Equipment Corp., Santa Barbara, CA) following recommendations by Turner (1988) and Koide et al. (1989). Leaves were previously covered with aluminum foil for ca. 2 h to allow the equilibrium between leaf Ψ and Ψ_x. Current-year shoot segments (30 mm long) were sampled and prepared as described above for *k* measurements using the XYL'EM® apparatus. The native and maximum *k* were determined by using a degassed and filtered (0.22 μm) 10 m*M* KCl solution at a hydrostatic pressure gradient of 3 kPa. Maximum *k* was measured similarly to native *k* but after removing embolism from the segments by flushing them with the same solution at a pressure of 0.15 MPa for 20 min. Previous experiments showed that this pressure and time were sufficient to remove the embolisms. PLC values were calculated by expressing native *k* as a percentage of maximum *k* (Sperry et al. 1988):

$$\text{PLC} = 100 \times \left(\frac{1 - \text{native } k}{\text{Maximum } k}\right) \quad (1)$$

These measurements were carried out at J.E. Fernandez's laboratory (IRNAS, Spain) in September 2010.

VCs by bench dehydration, pressure collar and centrifuge methods

For the bench dehydration method, the collected branches (sampling date: July 19, 2010) were allowed to dehydrate gradually in the laboratory. Prior to Ψ_x determinations, branches were sealed into a plastic bag with wet paper towel inside for a minimum of 2 h to allow the equilibrium between leaf Ψ and Ψ_x. Ψ_x was then determined in two leaves per branch with a Scholander-type pressure chamber. Mean PLC was determined as for native data (Eqn 1) in six 30-mm-long xylem current-year shoot segments per branch at different times during dehydration to increase the range of Ψ_x values evaluated. PLC data were then binned for each Ψ_x and curve fitted to the binned data. Measurements for the bench dehydration method were carried out at H. Cochard's laboratory (INRA, Clermont-Ferrand, France). For the pressure collar method, measurements were carried out on five 0.3-m-long current-year shoot segments from different trees (sampling date: July 2, 2010). After removing the leaves and bark, the leaf scars were sealed with glue (Loctite® 454, Henkel Corporation, Düsseldorf, Germany) and paraffin film. Each shoot was then inserted into a double-ended pressure chamber (Cochard et al. 1992) with both ends protruding and its basal end connected to the XYL'EM® apparatus. Thus, the pressurized air was applied in the 0.13-m-long central portion of the sample. The shoots were flushed at 0.15 MPa to remove the embolisms until a stable maximum *k* value was reached. The *k* measurements were done at a hydrostatic pressure gradient of 9 kPa to ensure a measurable flow. The VC was generated by pressuring the collar to a desirable target value for 10 min and, then, slowly lowering it to atmospheric pressure. After ca. 25 min to allow the sample to equilibrate, *k* was measured. This process was repeated for the following target pressures: 0.5, 1.25, 2.5, 3.75, 5.0, 6.25 and 7.5 MPa. PLC values were calculated (Eqn 1) for the resulting *k* values. These measurements were carried out at J.E. Fernández's laboratory (IRNAS, Spain).

For the static-centrifuge method, a 150-mm-diameter and a 280-mm-diameter custom-built rotor designed according to Alder et al. (1997) were used for performing the VCs from current-year shoot segments (n = 3–7) (sampling dates: July 26, 2010 and September 27, 2010, respectively). Samples were adjusted to the desired length with a razor blade and flushed at ca. 0.15 MPa to remove the embolism until a stable maximum *k* value was reached. They were then installed in the rotor and spun at different velocities for 2 min with their ends submersed into water to induce the desired tensions. After spinning, samples were removed from the rotor and immersed in tap water. Two 20- to 30-mm-long segments were then excised under water from the middle part of each sample and their *k* and PLC were determined as described for native embolism (Pockman et al. 1995, Cochard et al. 2010). Samples were exposed to each of the following tensions: 0.5, 1.0, 1.5, 2.0, 3.0, 4.0 and 5.0 MPa. PLC was calculated from the initial *k* and *k* after spinning at the tensions. These measurements were carried out at S. Mayr's laboratory (for the 150-mm rotor; University of Innsbruck, Innsbruck, Austria) and J.S. Sperry's laboratory (for the 280-mm rotor; University of Utah, Salt Lake City, UT).

Three VCs were generated with the flow-centrifuge method from current-year shoot segments: one in a 280-mm-diameter custom-built rotor designed according to Cochard et al. (2005) (Cavitron; measurements carried out at H. Cochard's laboratory); and two in the 150-mm-diameter and 280-mm-diameter custom-built rotors used for the static-centrifuge method but modified according to Li et al. (2008) to allow the *k* determination while spinning (measurements carried out at S. Mayr's laboratory and J.S. Sperry's laboratory, respectively). As for the static-centrifuge method, all samples used for flow-centrifuge measurements were adjusted to the desired length with a razor blade, flushed at ca. 0.15 MPa to remove any embolism until a stable maximum *k* value was reached and then installed in the corresponding rotor. Each sample was then spun at increasing speeds to get progressively higher xylem tensions while the variation on *k* was determined once that a stable flow was reached (Cochard et al. 2005, Li et al. 2008). A minimum of three samples were used for each VC. PLC was quantified as in Eqn 1.

All VCs were plotted as PLC vs xylem tension and fitted using a Weibull function (Neufeld et al. 1992) with an additional independent factor to consider the levels of embolism measured at $\Psi_x = 0$:

$$\mathrm{PLC} = \left(100 - y_0\right) - \left(100 - y_0\right) \mathrm{e}^{-(x/b)^c} + y_0 \qquad (2)$$

with x representing the xylem tension, b the xylem tension for a PLC of 63%, c a dimensionless parameter controlling the shape of the curve and y_0 the PLC at xylem tensions of 0 MPa. These points were fitted to Eqn 2 using Excel's solver function. For VCs obtained by pressure collar and centrifuge methods, y_0 was assumed to be zero as samples were flushed to remove all native embolisms before generating the VCs. The xylem tension inducing 50% loss of hydraulic conductance (P_{50}, MPa) due to cavitation and its 95% confidence intervals (CIs) were calculated from each VC.

HRCT imaging

Similar branches, collected as described above, were maintained in contact with water overnight to allow full rehydration. Then, they were dehydrated gradually and their Ψ_x determined at intervals as for the bench dehydration method. After measuring Ψ_x, 30-mm-long xylem segments were excised under water from current-year shoots as described above for *k* measurements and wrapped into a paraffin film in order to prevent drying during the X-ray scan. Samples were then placed in an X-ray microtomograph (Nanotom 180 XS, GE, Wunstorf, Germany) at the PIAF laboratory of the Institut National de la Recherche Agronomique (INRA, Clermont-Ferrand, France). X-ray scans provided three-dimensional images of the internal structure of the sample. The field of view was $3.2 \times 3.2 \times 3.2$ mm and covered the full cross section of the samples. X-ray source settings were 50 kV and 275 μA. For each 50-min scan, 1100 images were recorded during the 360° rotation of the sample. After 3D reconstruction, the spatial resolution of the image was $1.56 \times 1.56 \times 1.56$ μm per voxel. One transverse 2D slice was extracted from the middle of the volume using VGStudio Max© software (Volume Graphics, Heidelberg, Germany). Samples were then removed from the Nanotom, air-injected at both ends for 2 min at 0.9–1.0 MPa for filling all their vessels with air and placed again in the Nanotom for a new image acquisition. A total of seven samples from branches with Ψ_x from −0.3 to −8.5 MPa were used for generating the VC as described in the following.

The 2D images were then analyzed using IMAGEJ image analysis software (Version 1.47i, National Institutes of Health, Bethesda, MD) for determining the PLC of each sample following a similar protocol as that described by Brodersen et al. (2013). Briefly, the images were cropped to include only the xylem portion and then converted to a binary format for their analysis. The lumen areas and diameters of the non-functional vessels (i.e. air-filled) were determined and their volumetric flow rate was then calculated using the Hagen–Poiseuille equation. The PLC was determined (Eqn 1) based on the calculated maximum *k* of the entire population of vessels and the *k* of non-functional vessels at each Ψ_x. All spots with a diameter <4 μm were not considered for *k* calculations as a recent study carried out on the same trees and under the same conditions has reported no vessels with diameters lower than this value (Torres-Ruiz et al. 2013).

Maximum vessel length and vessel length distribution

Current-year shoots (>1 m long) were sampled from different representative trees and their embolism was removed by flushing for 1 h at ca. 0.15 MPa with the same solution as for *k* measurements. The maximum vessel length was determined in 20 branches by the air perfusion technique (Ewers and Fisher 1989). Briefly, each branch was infiltrated with compressed air at 0.05 MPa at its basal end while its apical end was immersed in water. The branch was successively shortened by 20 mm portions until air bubbles were seen. The remaining sample length was then considered equal to the maximum vessel length of the sample.

The vessel length distribution was estimated in five air-injected shoots by determining the PLC level at different distances from the injected shoot end (Cochard et al. 1994). For this, and after removing the embolism by flushing, shoots were air-injected at their basal ends at 0.1 MPa for 10 min. This pressure was low enough to avoid air flowing through wet pit membranes to adjacent vessels (Ewers and Fisher 1989). Thus, all vessels open at the base level became entirely air-filled. Segments of 50 mm in length were sampled under water every 100 mm, from the base to the apical end of each shoot, and their PLC determined as described for native embolism. Results were useful to estimate the vessel-length distribution of the samples as higher PLC levels are expected for a given distance as the proportion of open vessels increases toward the shoot base.

Maximum stem-specific hydraulic conductivity during the dehydration process

To test whether the maximum stem-specific hydraulic conductivity (K_s, kg m^{-1} s^{-1} MPa^{-1}) changes during the dehydration process, three to five branches (>1.5 m long) were collected from three different trees, transported to the laboratory and allowed to dehydrate gradually. Before collecting the samples, branches were wrapped into plastic bags with wet paper towel inside for at least 2 h (in order to prevent transpiration and to promote equilibration of leaf Ψ and Ψ_x), and their Ψ_x were then determined with a Scholander chamber in 4–5 leaves per branch. Maximum K_s was determined in three different sets of 30 mm shoot segments (n = 8–9 in each set) sampled just after harvesting, and 24 and 48 h after harvesting. Samples were collected and prepared as described above to determine their k with a XYL'EM® apparatus. The maximum k was determined after flushing the samples to remove the embolism (as described for native embolism measurements), divided by the base cross-section (pith included) and multiplied by the sample length to calculate the maximum K_s.

Statistics

The lower and upper CIs of P_{50} values were used to determine whether they were significantly different between methods used for generating the VCs. Maximum vessel length data are given as mean ± standard error and differences were considered to be significant if $\alpha \leq 0.001$. Differences in maximum K_s between groups of current-year shoot segments collected at different times were tested by a one-way repeated measures analysis of variance and they were considered to be significant if $\alpha \leq 0.05$. Dixon's test was used to determine outliers (Sokal and Rohlf 1995). CIs (95%) of the VCs were computed based on the sample mean and sample standard deviation (reduced chi-square method). Analyses were made with Sigmaplot 11.0 (Systat Software, Inc., San Jose, CA).

Results

Native PLC and vulnerability to cavitation

The native PLC ranged from 11 to 33% for a Ψ_x range of −1.6 to −3.6 MPa (Fig. 1A). The VCs obtained from dehydrated samples, i.e. using the bench dehydration method and HRCT (see Fig. 2 for the transverse HRCT micrographs), were 's'-shaped, whereas the pressure collar and the centrifuge methods yielded 'r'-shaped VCs (Fig. 1). The bench dehydration and HRCT VCs showed similar P_{50} values of 5.0 and 4.4 MPa, respectively (Table 1). The VCs resulting from the pressure collar (Fig. 1B) and from the static-centrifuge (Fig. 1C) methods using the 280-mm-diameter rotor showed similar vulnerability to cavitation and P_{50} values of 3.7 and 2.8 MPa, respectively. The static-centrifuge method reported higher vulnerability to cavitation when VCs were generated with the smaller rotor and, therefore, from shorter samples ($P_{50} = 0.9$ MPa, Table 1). The two 280-mm-diameter rotor designs used for flow-centrifuge measurements revealed similar P_{50} values (Fig. 1D).

Maximum K_s during dehydration

No significant differences in maximum K_s were found between xylem segments sampled at different times during the dehydration process (Fig. 3). Segments sampled after harvesting showed a mean Ψ_x value of -0.82 ± 0.08 MPa and a mean maximum K_s value of 0.82 ± 0.07 kg MPa^{-1} s^{-1} m^{-1}. Samples collected 24 and 48 h after harvesting showed mean Ψ_x values of -4.45 ± 0.24 and -6.91 ± 0.22 MPa and mean maximum K_s values of 0.68 ± 0.09 and 0.81 ± 0.10 kg MPa^{-1} s^{-1} m^{-1}, respectively.

Maximum vessel length and PLC levels along air-injected shoots

The air perfusion technique revealed values of maximum vessel length of 0.819 ± 0.015 m (SE; n = 20). The shoots injected with air at low pressure showed vessels open at 1 m from the base of the shoot (Fig. 4). Fig. 4 also indicates that a fraction of vessels would be open at both ends in 150-mm-long and 280-mm-long xylem samples as, at such distances from the injected shoot end, the PLC levels were around 70 and 50%, respectively.

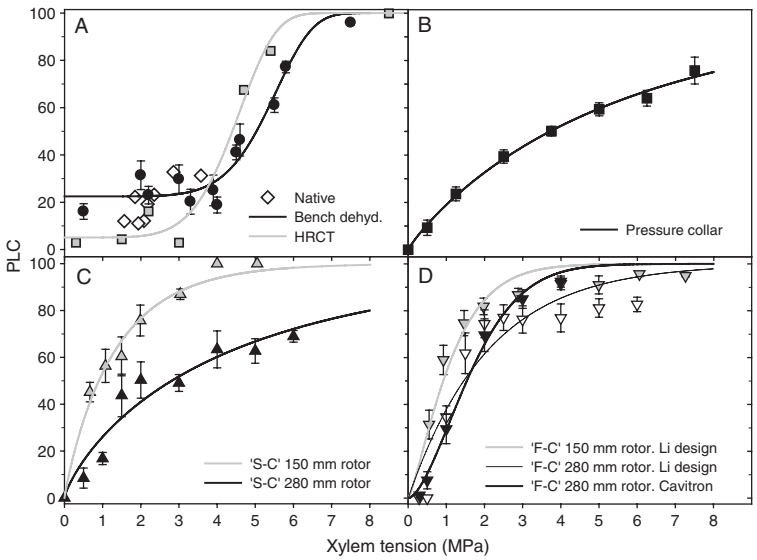

Fig. 1. (A) Native embolism (white diamonds) and VCs to cavitation based on PLC data on olive current-year shoots generated by bench dehydration (black circles) and HRCT (gray squares); (B) VCs generated with the pressure collar method (black squares), n = 5; (C) VCs generated by the static-centrifuge method ('S-C') in a 150-mm-diameter rotor (gray triangles, gray line) and in a 280-mm-diameter rotor (black triangles, black line), n = 3–7; (D) VCs generated with the flow-centrifuge method ('F-C') in a 150-mm-diameter rotor (gray triangles, gray line) and in a 280-mm-diameter rotor (white triangles, thin black line) designed according to Li et al. (2008), and in a 280-mm-diameter Cavitron (black triangles, thick black line), n > 3. Each point indicates the mean PLC ± standard error (vertical bars) at different xylem tensions. Details about methods are given in the text.

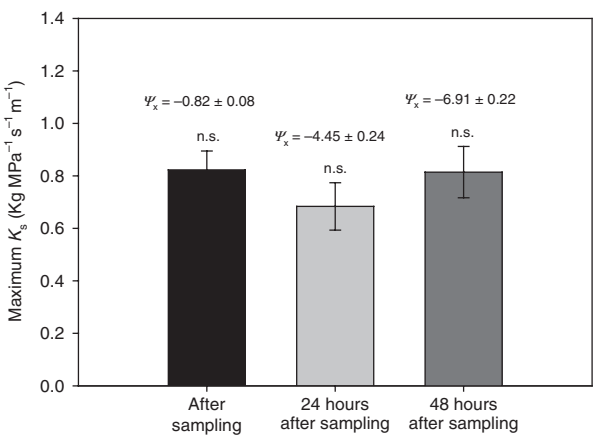

Fig. 2. Maximum stem-specific hydraulic conductivity (K_s, kg m^{-1} s^{-1} MPa^{-1}) determined in three different sets of 30-mm current-year shoot segments (n = 8–9 in each set) collected from three to five big branches (>1.5 m long) at different times during their dehydration. Measurements in group 'a' were carried out after the collection of branches and in group 'b' and 'c' 24 and 48 h after the collection of branches, respectively. Columns indicate the mean maximum K_s (n = 8–9) ± standard error. Ψ_x indicates the mean xylem water potential ± standard error (MPa, n = 4–5) of the branches before collecting the shoot segments for each group of measurements. n.s. = no significant difference.

Discussion

Results showed that different vulnerabilities to cavitation were obtained depending on the method and the sample length used for generating the VCs. The VCs obtained from dehydrated samples, i.e. using the bench dehydration method and HRCT, indicated higher resistances to cavitation than those obtained using the pressure collar or the centrifugation methods (Fig. 1; Table 1). VCs resulting from bench dehydration showed a range of xylem tensions (from 0 to ca. 3 MPa) where PLC remained low and nearly constant up to a critical xylem tension (3–4 MPa) at which PLC increased rapidly ('s'-shaped VCs). Results obtained by using HRCT showed even lower PLC values at low xylem tensions than the bench dehydration curve and than the native PLC values. This may be due to the full rehydration of the samples before use in HRCT experiments. However, both curves showed similar P_{50} values. On the contrary, the pressure collar and centrifuge VCs exhibited relevant losses in k at xylem tensions already near 0.5 MPa ('r'-shaped VC), which suggests that the resistance to cavitation was underestimated. Sigmoidal VCs have been previously reported for olive shoots using the bench dehydration method and they showed P_{50} values similar to those reported by the dehydration curves of this study (Ennajeh et al. 2008, Torres-Ruiz et al. 2013).

In agreement with our results, Ennajeh et al. (2011) also reported overestimated vulnerabilities to cavitation with the pressure collar method when the sample length minus the chamber length was lower than the maximum vessel length, as it was in our case. This is consistent

Table 1. Xylem tension inducing 50% loss of hydraulic conductance (P_{50}) with the 95% CI, fit equation parameters calculated from the VCs derived from Eqn 2 and sampling dates for each method used (see text for details). P_{50} values whose 95% CI do not overlap are considered significantly different (different letters). The column 'Lab' indicates the laboratory in which the measurements were carried out: (i), H. Cochard's lab; (ii), J.E. Fernández's lab; (iii), S. Mayr's lab; (iv), J. Sperry's lab.

Method	Rotor diameter (mm)	P_{50} (MPa) (95% CI)	Fit equation parameters			Sampling	Lab
			b	c	y_0		
Bench dehydration		5.0 (4.69; 5.32)a	5.7	6.8	22.5	July 2010	i
Pressure collar		3.7 (3.49; 3.96)bd	5.6	0.9	0	July 2010	ii
Static-centrifuge	150	0.9 (0.71; 1.15)c	1.3	0.9	0	July 2010	iii
	280	2.8 (2.18; 3.56)b	4.4	0.8	0	September 2010	iv
Flow-centrifuge	150 Li design	0.9 (0.69; 1.15)c	1.2	1.3	0	July 2010	iii
	280 Li design	1.5 (0.95; 2.16)ce	2.1	1.0	0	September 2010	iv
	280 Cavitron	1.5 (1.34; 1.73)e	1.9	1.6	0	July 2010	i
HRCT		4.4 (3.75; 4.94)ad	4.7	5.8	5.1	February 2013	i

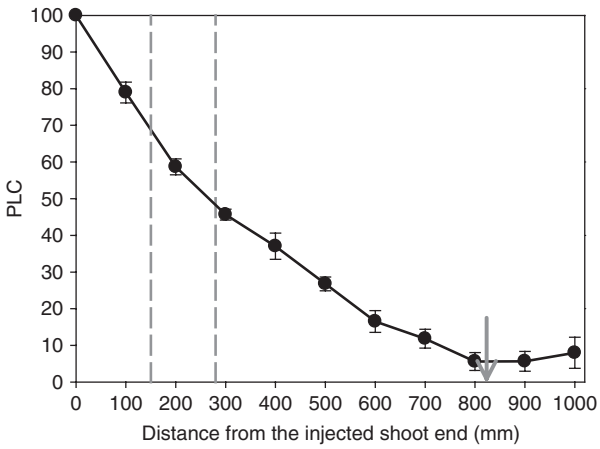

Fig. 3. Mean PLC (n = 5) in air-injected shoots at different distances from the injected shoot end. Vertical bars represent the standard error. The gray dashed lines indicate the two sample lengths used for the centrifuge methods (150 and 280 mm). The arrow indicates the maximum vessel length determined by the air perfusion technique (see text for details).

with Martínez-Vilalta et al. (2002), who suggested that the high vulnerabilities in relation to the field water potentials reported for *Quercus* stems were probably due to the very long vessels of the species, causing artifacts with the pressure collar method.

Results obtained from the static-centrifuge method (Fig. 1C) also indicate an effect of the portion of open vessels at both sample ends on the VC, given that greater vulnerabilities to cavitation, i.e. significant lower P_{50} values, were obtained from 150-mm samples than from 280-mm samples (Table 1). This results from shorter samples having higher fraction of open vessels than longer samples (Fig. 4) that cavitate at lower xylem tensions than intact ones (Choat et al. 2010).

Our results are also in agreement with a recent study published by Cochard et al. (2013) in which they evaluated the shape of 867 VCs distributed across techniques. Their results showed that 'r'-shaped curves were strongly associated with pressure collar and centrifugation methods and the presence of large conduits in the xylem. By contrast, curves obtained with the bench dehydration method were 's'-shaped as a rule. Previous studies in olive (Moriana et al. 2002, Fernández et al. 2006, Gómez-del-Campo et al. 2008) have shown that well-irrigated and moderately water-stressed trees keep their minimum stem Ψ between −1.5 and −2.0 MPa, which suggests an isohydric behavior in olive. The homeostasis in Ψ, i.e. isohydric behavior, can be explained by hydraulic factors exclusively if the plant is operating close to the cavitation threshold (Buckley 2005). It is unlikely, therefore, that a plant can risk 70% PLC during normal transpiration conditions as 'r'-shaped curves suggest, especially if the stomatal control of transpiration is aimed to avoid a large runway cavitation and to maintain its hydraulics (Choat et al. 2012).

Our results contrast with the results reported by Sperry et al. (2012) on several species, including olive, who observed that curves obtained with the static-centrifuge method were relatively insensitive to the number of open vessel of the samples. This discrepancy between results in olive could be based on differences in sample age and, in consequence, on effects of cavitation fatigue (Hacke et al. 2001) and on previous damages in the vessel end-walls ('leaks'), which would increase the vulnerability to cavitation of the samples. Contrasting results regarding the reliability of the centrifuge methods have also been reported for other long-vesseled species such as *V. vinifera*. Thus, whereas Jacobsen and Pratt (2012) and Tobin et al. (2013) found no evidence for an artifact associated with open vessels, McElrone et al. (2012) reported that the centrifuge method consistently overestimates vulnerability to cavitation in this species. Different vulnerabilities to cavitation have also been

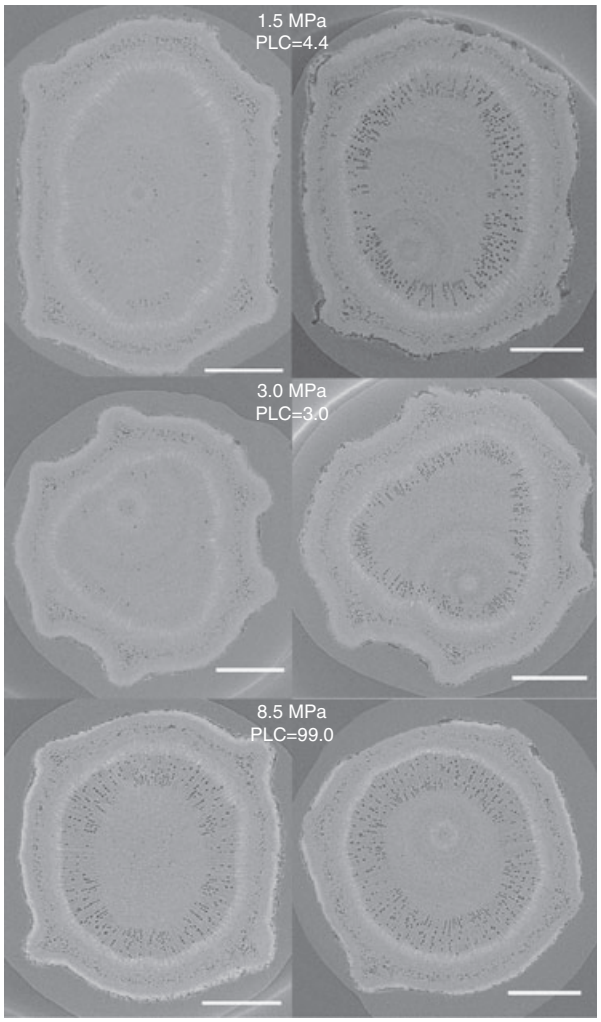

Fig. 4. Transverse HRCT micrographs of *Olea europaea* current-year shoots at different xylem tensions. Images show the amount of cavitated or air-filled conduits at each xylem tension before (left) and after (right) the air injection of the samples. Cavitated or air-filled vessels are observed as black. Xylem water tension and PLC are indicated for each sample. Scale bars = 500 μm.

obtained for the flow-centrifuge method when using different rotor designs, being these ascribed to differences in the method of water delivery between the two rotor designs (Sperry et al. 2012). In our case, the flow-centrifuge method reported higher PLC values than the methods based on dehydration and native data, regardless of rotor design and size (Fig. 1D). With both centrifuge methods, vulnerability thresholds increased as the sample length decreased, suggesting an open-vessel artifact with these methods. There are several possible explanations for this open-vessel artifact including water draining from open vessels when the centrifuge starts spinning (Choat et al. 2010), or cavitation seeding by microscopic particles/air bubbles when flow is induced across the samples or on flushing (Cochard et al. 2005). However, our experiments did not focus on the cause of such higher vulnerabilities, but rather its consequences for the accuracy of the VCs in olive specifically and, probably, in other species with similar xylem characteristics (i.e. long vessels).

Although the bench dehydration method has been used for generating 'reference curves' in different studies (Cochard et al. 2010, Ennajeh et al. 2011), it is not exempt from possible issues caused, e.g. by an incomplete embolism removal, changes in maximum k because of vessel inactivation or cutting artifacts (Wheeler et al. 2013). Jacobsen and Pratt (2012) observed in *Vitis* significant declines in maximum K_s apparently caused by the formation of gels within the vessel of dehydrated shoots. These declines in maximum K_s were not observed during the dehydration in our study with olive as shoot segments showed similar maximum K_s at the sampling day and after 24 and 48 h of dehydration. This time was long enough to decrease the Ψ_x of the branches from −0.82 to −6.91 MPa and, therefore, to generate a VC by bench dehydration. Also, no changes in maximum K_s during the dehydration were observed in a similar study carried out in current-year shoot segments from the same trees used in this study (unpublished; Fig. S1, Supporting Information). In addition, the agreement between the VCs obtained with the bench dehydration method and by HRCT also indicates no xylem blockages during the dehydration process. Therefore, a plugging problem cannot explain the discrepancy between these two sets of curves.

Additional insights may be provided when VCs are based on absolute conductivity values. However, although K_s is proportional to the section of conducting wood (Cruiziat et al. 2002), previous studies on olive current-year shoots have reported a high scattering in the maximum hydraulic conductivity (K) vs wood cross-sectional relationship (Fig. S2). Thus, samples with similar wood cross-sectional areas would show very different maximum k values. This, therefore, creates a higher level of uncertainty associated with K_s data compared with relative PLC values. In addition, for determining absolute K values properly, it is important that the measured segment be long relative to the length of a typical vessel as open vessels at both ends can provide a high conductance path that would lead to significant errors in the estimation of K (Melcher et al. 2012). As the methods evaluated in this study required the use of very different sample lengths, the total amount of open vessels at both ends would also be different between them, complicating the use of K absolute values for a proper comparison of the methods.

According to these results, we conclude that the bench dehydration method yielded the most reliable VC for olive current-year shoots, as shown by the good agreement with native PLC data and the HRCT results. Both the pressure collar and the two tested centrifuge methods (static- and flow-centrifuge), regardless of rotor design, overestimated the vulnerability to cavitation of this long-vesseled species, reporting higher PLC values than those determined from trees under field conditions. Both the static- and flow-centrifuge methods reported different vulnerability to cavitation depending on the sample length and, therefore, the proportion of open vessels in the sample, supporting the open-vessel artifact hypothesis.

Acknowledgements – We thank Prof. John S. Sperry, University of Utah (Salt Lake City, UT, USA), for discussions and comments on manuscript drafts. Alberto Vilagrosa contributed greatly to the discussion of results. We thank the Spanish Ministry of Science and Innovation (research projects AGL2006-04666/AGR and AGL2009-11310/AGR) and the Austrian Science Fund (FWF) (P20852-B16 and L 556-B16) for funding this work. J. M. T.-R. held a doctoral fellowship from the Spanish Ministry of Science and Innovation (BES-2007-17149, MCINN). We thank Antonio Montero for helping us with the sample collection.

References

Alder NN, Pockman WT, Sperry JS, Nuismer S (1997) Use of centrifugal force in the study of xylem cavitation. J Exp Bot 48: 665–674

Allen R, Pereira LS, Raes D, Smith M (1998) Crop evapotranspiration. Guidelines for computing crop water requirements. Irrigation and Drainage Paper, No. 56. FAO, Rome.

Barranco D, Fernández-Escobar R, Rallo L (1998) The Culture of the Olive Tree. Mundi-Prensa, Madrid

Brodersen CR, McElrone AJ, Choat B, Lee EF, Shackel KA, Matthews MA (2013) In vivo visualizations of drought-induced embolism spread in *Vitis vinifera*. Plant Physiol 161: 1820–1829

Buckley TN (2005) The control of stomata by water balance. New Phytol 168: 275–292

Charra-Vaskou K, Badel E, Burlett R, Cochard H, Delzon D, Mayr S (2012) Hydraulic efficiency and safety of vascular and non-vascular components in *Pinus pinaster* leaves. Tree Physiol 32: 1161–1170

Choat B, Drayton WM, Brodersen C, Matthews MA, Schackel KA, Wada H, McElrone AJ (2010) Measurement of vulnerability to water stress-induced cavitation in grapevine: a comparison of four techniques applied to a long-vesseled species. Plant Cell Environ 33: 1502–1512

Choat B, Jansen S, Brodribb TJ, Cochard H, Delzon S, Bhaskar R, Bucci SJ, Feild TS, Gleanson SM, Hacke UG, Jacobsen AL, Lens F, Maherali H, Martinez-Vilalta J, Mayr S, Mencuccini M, Mitchel PJ, Nardini A, Pittermann J, Pratt RB, Sperry JS, Westoby M, Wright IJ, Zanne AE (2012) Global convergence in the vulnerability of forests to drought. Nature 491: 752–755

Cochard H (2002) A technique for measuring xylem hydraulic conductance under high negative pressures. Plant Cell Environ 25: 815–819

Cochard H, Cruiziat P, Tyree M (1992) Use of positive pressures to establish vulnerability curves. Plant Physiol 100: 205–209

Cochard H, Ewers FW, Tyree MT (1994) Water relations of a tropical vine-like bamboo (*Rhipidocladum racemiflorum*). Root pressures, vulnerability to cavitation and seasonal changes in embolism. J Exp Bot 45: 1085–1089

Cochard H, Damour G, Bodet C, Tharwat I, Poirier M, Ameglio T (2005) Evaluation of a new centrifuge technique for rapid generation of xylem vulnerability curves. Physiol Plant 124: 410–418

Cochard H, Herbette S, Barigah T, Vilagrosa A (2010) Does sample length influence the shape of vulnerability to cavitation curves? A test with the Cavitron spinning technique. Plant Cell Environ 33: 1543–1552

Cochard H, Badel E, Herbette S, Delzon S, Choat B, Jansen S (2013) Methods for measuring plant vulnerability to cavitation: a critical review. J Exp Bot 64: 4779–4791

Cruiziat P, Cochard H, Améglio T (2002) The hydraulic architecture of trees: main concepts and results. Ann For Sci 59: 723–752

Ennajeh M, Tounekti T, Ahmedou MV, Khemira H, Cochard H (2008) Water relations and drought-induced embolism in two olive (*Olea europaea* L.) varieties 'Meski' and 'Chemlali' under severe drought conditions. Tree Physiol 28: 971–976

Ennajeh M, Simoes F, Khemira H, Cochard H (2011) How reliable is the double-ended pressure sleeve technique for assessing xylem vulnerability to cavitation in woody angiosperms? Physiol Plant 142: 205–210

Ewers FW, Fisher JB (1989) Techniques for measuring vessel lengths and diameters in stems of woody plants. Am J Bot 76: 645–656

Fernández JE, Diaz-Espejo A, Infante JM, Durán P, Palomo MJ, Chamorro V, Girón IF, Villagarcía L (2006) Water relations and gas exchange in olive trees under regulated deficit irrigation and partial rootzone drying. Plant Soil 284: 273–291

Franks P, Brodribb TJ (2005) Stomatal control and water transport in the xylem. In: Holbrook NM, Zwieniecki MA (eds) Vascular Transport in Plants. Academic Press, Amsterdam, the Netherlands, pp 69–89

Gómez-del-Campo M, Leal A, Pezuela C (2008) Relationship of stem water potential and leaf

conductance to vegetative growth of young olive trees in a hedgerow orchard. Aust J Agric Res 59: 270–279
Hacke UG, Stiller V, Sperry JS, Pittermann J, McCulloh KA (2001) Cavitation fatigue: embolism and refilling cycles can weaken cavitation resistance of xylem. Plant Physiol 125: 779–786
Jacobsen AL, Pratt RB (2012) No evidence for an open vessel effect in centrifuge-based vulnerability curves of a long-vesseled liana (*Vitis vinifera*). New Phytol 194: 982–990
Koide RT, Robichaux RH, Morse SR, Smith CM (1989) Plant water status, hydraulic resistance and capacitance. In: Pearcy RW, Ehleringer J, Mooney HA, Rundel PW (eds) Plant Physiological Ecology. Chapman & Hall, London, pp 161–179
Li Y, Sperry JS, Bush SE, Hacke UG (2008) Evaluation of centrifugal methods for measuring xylem cavitation in conifers, diffuse- and ring-porous angiosperms. New Phytol 177: 558–568
Martínez-Vilalta J, Prat E, Oliveras I, Piñol J (2002) Xylem hydraulic properties of roots and stems of nine Mediterranean species. Oecologia 133: 19–29
Mayr S, Rothart B, Wolfschwenger M (2006) Temporal and spatial pattern of embolism induced by pressure collar techniques in twigs of *Picea abies*. J Exp Bot 57: 3157–3163
McElrone AJ, Brodersen CR, Alsina MM, Drayton WM, Matthews MA, Shackel KA, Wada H, Zufferey V, Choat B (2012) Centrifuge technique consistently overestimates vulnerability to water stress-induced cavitation in grapevines as confirmed with high-resolution computed tomography. New Phytol 196: 661–665
Melcher PJ, Holbrook NM, Burns MJ, Zwieniecki MA, Cobb AR, Brodribb TJ, Choat B, Sack L (2012) Measurements of stem xylem hydraulic conductivity in the laboratory and field. Methods Ecol Evol 3: 685–694
Moriana A, Villalobos FJ, Fereres E (2002) Stomatal and photosynthetic responses of olive (*Olea europaea* L.) leaves to water deficits. Plant Cell Environ 25: 395–405
Neufeld HS, Grantz DA, Meinzer FC, Goldstein G, Crisosto GM, Crisosto C (1992) Genotypic variability of leaf xylem cavitation in water-stressed and well-irrigated sugarcane. Plant Physiol 100: 1020–1028
Pastor M (2005) Cultivo del olivo con riego localizado. Junta de Andalucia, Consejería de agricultura y pesca & Mundi-Prensa.
Pockman WT, Sperry JS, O'Leary JW (1995) Evidence for sustained and significant negative pressure in xylem. Nature 378: 715–716
Salleo S, Hinckley TM, Kikuta SB, Lo Gullo MA, Weilgony P, Yoon TM, Richter H (1992) A method for introducing xylem embolism *in situ* – experiments with a field grown tree. Plant Cell Environ 15: 491–497
Sokal RR, Rohlf FJ (1995) Biometry, 3rd Edn. W.H. Freeman, New York
Sperry JS, Saliendra NZ (1994) Intra- and inter-plant variation in xylem cavitation in *Betula occidentalis*. Plant Cell Environ 17: 1233–1241
Sperry JS, Tyree MT (1988) Mechanism of water stress-induced xylem embolism. Plant Physiol 88: 581–587
Sperry JS, Donnelly JR, Tyree MT (1988) A method for measuring hydraulic conductivity and embolism in xylem. Plant Cell Environ 11: 35–40
Sperry JS, Christman MA, Torrez-Ruiz JM, Taneda H, Smith DD (2012) Vulnerability curves by centrifugation: is there an open vessel artefact, and are "r" shaped curves necessarily invalid? Plant Cell Environ 35: 601–610
Taneda H, Sperry JS (2008) A case-study of water transport in co-occurring ring- versus diffuse-porous trees: contrasts in water-status, conducting capacity, cavitation and vessel refilling. Tree Physiol 28: 1641–1652
Tobin MF, Pratt RB, Jacobsen AL, De Guzman M (2013) Xylem vulnerability to cavitation can be accurately characterized in species with long vessels using a centrifuge method. Plant Biol 15: 496–504
Torres-Ruiz JM, Diaz-Espejo A, Morales-Sillero A, Martín-Palomo MJ, Mayr S, Beikircher B, Fernández JE (2013) Shoot hydraulic characteristics, plant water status and stomatal response in olive trees under different soil water conditions. Plant Soil 373: 77–87
Turner NC (1988) Measurement of plant water status by the pressure chamber technique. Irrig Sci 9: 289–308
Tyree MT, Zimmermann MH (2002) Xylem Structure and the Ascent of Sap, 2nd Edn. Springer-Verlag, Berlin
Wheeler JK, Huggett BA, Tofte AN, Rockwell FE, Holbrook NM (2013) Cutting xylem under tension or supersaturated with gas can generate PLC and the appearance of rapid recovery from embolism. Plant Cell Environ 36: 1938–1949

Supporting Information

Additional Supporting Information may be found in the online version of this article:

Fig. S1. Maximum stem-specific hydraulic conductivity (maximum K_s) values in xylem segments of olive current-year shoots from a bench dehydration VC generated in 2010 by J. M. Torres-Ruiz.

Fig. S2. Relationship between the maximum hydraulic conductivity (maximum K) and the cross-sectional area of 30 mm current-year shoot segments.